Nucleation of nitric acid hydrates in Polar Stratospheric Clouds by meteoric material

Alexander D. James[1], James S. A. Brooke[1], Thomas P. Mangan[1], Thomas F. Whale[2], John M. C. Plane[1], and Benjamin J. Murray[2]

[1] School of Chemistry, University of Leeds, Leeds LS2 9JT, UK.
[2] School of Earth and Environment, University of Leeds, Leeds LS2 9JT, UK.

Correspondence regarding PSCs and nucleation experiments to: Benjamin J. Murray (B.J.Murray@leeds.ac.uk)

Correspondence regarding meteoric material and WACCM simulations to: John M. C. Plane (J.M.C.Plane@leeds.ac.uk)

Abstract. Heterogeneous nucleation of crystalline nitric acid hydrates in Polar Stratospheric Clouds (PSCs) enhances ozone depletion. However, the identity and mode of action of the particles responsible for nucleation remains unknown. It has been suggested that meteoric material may trigger nucleation of nitric acid trihydrate (NAT), but this has never been directly demonstrated in the laboratory. Meteoric material is present in two forms in the stratosphere, smoke which results from the ablation and re-condensation of vapours, and fragments which result from the disruption of meteoroids entering the atmosphere. Here we show that analogues of both materials have a capacity to nucleate nitric acid hydrates. In combination with estimates from a global model of the amount of meteoric smoke and fragments in the polar stratosphere we show that meteoric material probably accounts for NAT observations in early season polar stratospheric clouds in the absence of water ice.

1 Introduction

Polar Stratospheric Clouds (PSCs) catalyse the activation of Cl and Br species, which in turn catalytically destroy ozone (Solomon, 1999). The phase (liquid droplets or crystals) of PSC aerosol is particularly important: firstly, because rates of activation of Cl and Br species are different depending on the PSC phase; and secondly, because of denitrification where crystals of Nitric Acid Trihydrate (NAT) grow and sediment out of the stratosphere, removing HNO_3 and thus preventing formation of the inactive $ClONO_2$ reservoir (Wegner et al., 2012). Nucleation of NAT has been shown to be a major uncertainty in modelling of polar ozone (Brakebusch et al., 2013).

The mechanism and kinetics of nucleation of crystalline PSCs has been a long-standing question (Peter and Grooß, 2012). Nucleation on crystalline water ice is known to be a significant pathway in air masses affected by significant gravity wave activity, which causes rapid cooling. Up to 80 % of denitrification in the Arctic winter of 1999/2000 can be explained by this water ice mechanism (Mann et al., 2005). However, clouds are commonly observed under conditions where water ice is not stable (and has not been so within tens of hours) (Lambert et al., 2016; Voigt et al., 2005). There is also the possibility that Nitric Acid Dihydrate (NAD) may form initially, then transform to NAT (Grothe et al., 2008).

In cases where water ice is not present, an empirical Classical Nucleation Theory (CNT) parameterisation of heterogeneous nucleation on meteoric material gave good agreement with observed clouds (Hoyle et al., 2013). This agreement contrasts with the commonly used approach of assuming a constant nucleation rate in all air masses where NAT is stable, which is able to reproduce some observations but lacks predictive capability since it has no physical basis. Such a predictive capability of

5   nucleation in PSCs and resulting ozone depletion would require characterisation of heterogeneous nucleation kinetics on the appropriate atmospheric material, presumed to be of meteoric origin.

Several previous studies have examined the nucleating ability of analogues for meteoric material. In one case, ground micrometeorite suspended in aqueous nitric acid solutions did not produce observable nucleation (Biermann et al., 1996). The limiting rate of nucleation was not rapid enough to explain PSCs with high number densities, although it was later pointed out

10   that the limiting values were not sufficiently low to rule out nucleation in the atmosphere (Hoyle et al., 2013). It has also been noted that meteoric material will at least partially dissolve in acidic droplets, leaving silica materials undissolved (Bogdan et al., 2003;Saunders et al., 2012). It has been found that fumed silica was active as a heterogeneous nucleus of nitric acid hydrates under stratospheric conditions (Bogdan et al., 2003), but no quantification of the atmospheric implications of the measurements was made.

15   Two forms of meteoric material may be present in the stratosphere, with distinct composition and morphology; Meteoric Smoke Particles (MSPs) and meteoric fragments (MFs). MSPs, which form in the mesosphere from the metallic vapours injected by ablating meteoroids (Langowski et al., 2015), are too small to sediment gravitationally and are transported by the residual atmospheric circulation, taking 4-5 years to reach the Earth's surface (Dhomse et al., 2013). As a result of this relatively slow transport MSPs are entrained in sulfate aerosol below 35 km (Neely et al., 2011), causing the dissolution of

20   their metallic components over a period of several weeks (Saunders et al., 2012). It has been shown that the metallic content of meteoric materials is present in solution in mid-latitude stratospheric sulfate aerosol, whilst Si and Al components remain as solid inclusions (Murphy et al., 2014). Amorphous silica is therefore likely to be a useful analogue for MSPs partially dissolved in stratospheric sulfate. Fumed silica is particularly appropriate since its fractal morphology is probably similar to that of MSPs (Saunders and Plane, 2006).

25   A recent study (Carrillo-Sánchez et al., 2016) using the measured fluxes of Na and Fe in the upper mesosphere, and the deposition rate of cosmic spherules at the South Pole, concluded that 43 ± 14 tonnes of cosmic dust enters the atmosphere each day, of which 8 tonnes ablates and goes on to form MSPs. The remaining 35 tonnes of unablated particles, with radii $> 10\,\mu m$, are large enough to sediment rapidly into the troposphere. However, a recent study (Subasinghe et al., 2016) using high resolution video cameras found that 95 % of meteoroids larger than 1 mm fragmented on atmospheric entry. It was speculated

30   in that study that refractory silicate grains in the meteoroids are held together by a relatively volatile material which evaporates at temperatures significantly below those required to produce thermal ablation of the silicates. This would then result in a significant mass of unablated MFs. If these were submicron size then their slow rate of sedimentation in the lower stratosphere would allow them to influence PSC nucleation. In fact, single particle mass spectrometry measurements of 0.5 wt% Fe in

midlatitude sulfate aerosol indicated a meteoric input of 22 to 88 tonnes day^{-1}(Cziczo et al., 2001), suggesting the presence of meteoric material other than MSPs.

Here we investigate whether MSPs and / or MFs could provide a heterogeneous nucleation pathway to NAT in PSCs, as shown schematically in Figure 1. Heterogeneous nucleation activities were measured in the laboratory using a drop freezing assay technique (Whale et al., 2015), and then compared to other parameterisations of heterogeneous nucleation in PSCs and atmospheric observations of crystal particle concentrations (Voigt et al., 2005). To carry out these experiments, a range of analogues were chosen for MSPs and MFs. Since MFs are expected to undergo little to no ablation (Taylor et al., 2012), or dissolution of metals in acid droplets (since their sedimentation speed means that they have a short lifetime above the lower stratosphere), they are likely to have compositions similar to interplanetary dust and therefore were represented here by a range of ground meteorite analogues (James et al., 2017). MSPs in the mesosphere can be represented by amorphous materials of olivine composition (James et al., 2017); however, the significant time MSPs spend in acid droplets will cause dissolution of their metallic content (Saunders et al., 2012; Wise et al., 2003). MSPs were therefore represented here by amorphous silica analogues; fumed silica because of its fractal morphology, and fused quartz to test whether the results can be generalised to other forms of amorphous silica.

2 Methods

Drop freeze assays were performed using a modified version of a method we have described previously (Whale et al., 2015). Aqueous suspensions of heterogeneous materials were sonicated for one hour to break up aggregated material, shaken by hand (to ensure material was suspended evenly) and immediately used to dilute HNO_3 to the desired concentrations. Repeat experiments showed that this method gave reproducible nucleation activities, suggesting that particles were fully suspended. Mechanical stirring with magnetic stirrer bars was not applied as this was found to introduce contamination which induced nitric acid hydrate nucleation. A concentration of 39.94 ± 0.08 wt% (uncertainties given are 95 % confidence intervals) HNO_3 was used since this saturation ratio at stratospheric temperatures is relevant to synoptic PSCs. HNO_3 concentrations higher than about 45 wt% are not thought to be relevant to the atmosphere in the absence of gravity wave-induced temperature perturbations (Meilinger et al., 1995), whilst lower concentrations lead to nucleation under conditions where water ice is stable, also not relevant to the synoptic clouds we focus on here (Mann et al., 2005). Control experiments were carried out in which samples of H_2O were treated exactly as suspensions, including sonication and mixing with nitric acid. These control experiments were critical for minimising contamination and were routinely performed prior to experiments with the meteoric proxies.

Droplets were then pipetted onto a silanised glass slide, surrounded by a spacer (greased Viton o-ring) and covered with a second glass slide. The restricted volume provided by this sealed cell reduced the possible change in HNO_3 concentration due to evaporation or condensation to less than 1 wt% as predicted by a model of equilibrium vapour pressures (Clegg et al., 1998). The cell was situated on an aluminium block with an embedded PT100 thermocouple, on top of the EF600 cooling stage

(Whale et al., 2015). Comparison of the EF600 internal temperature probe with this calibrated PT100 show a maximum difference of <1 K at base temperature (183 K). Droplet arrays were made up with the surface held at 291 K to avoid condensation of atmospheric H_2O. Samples were then cooled at 5 K min^{-1} to 233 K followed by a 1 K min^{-1} cooling ramp to 183 K and a 3 K min^{-1} warming ramp to 248 K to observe melting. The onset of melting (see Sect. 3) was in agreement with

5 the ice I_h / NAT eutectic, giving further confidence in the temperature control and measurement. The sample cell was placed inside a larger cell which was flushed with dry N_2, zero grade: BOC, during the rapid cooling phase, then sealed to prevent frost formation on the outside of the sample cell. Figure 2 includes a schematic diagram and camera image (room temperature panel).

Samples were selected and their BET surface areas measured as analogues for both MSPs (Fused Quartz: 4.85 ± 0.06 m^2 g^{-1},

10 Fumed Silica: 195 ± 3 m^2 g^{-1}, $MgFeSiO_4$: 208 ± 2 m^2 g^{-1}) and MFs (NWA 2502 (CV3): 5.75 ± 0.05 m^2 g^{-1}, Chergach (H5): 0.44 ± 0.14 m^2 g^{-1}, Allende (CV3): 1.22 ± 0.15 m^2 g^{-1}). Fused quartz powder (r<43 µm) was purchased from Goodfellow Ltd. and used as supplied (without further grinding). Fumed silica (BET surface area 200 m^2 g^{-1}) was purchased from Sigma and used as supplied. $MgFeSiO_4$ was synthesised from chemical precursors using a sol-gel method we have described previously (James et al., 2017), and ground on an agate pestle. These samples cover a range of particles with the chemical and crystalline

15 characteristics of MSPs ($MgFeSiO_4$), the fractal agglomerate morphology of MSPs (fumed silica), and the chemical composition of MSPs after partial dissolution in acid droplets (fused quartz and fumed silica). SiO_2 materials were characterised in terms of their crystalline, morphological and elemental composition. Powder X-ray diffraction was used to show that the two SiO_2 materials contain no measurable crystalline component, as shown in the Supplementary Information (SI). Scanning Electron Microscopy with Energy Dispersive Electron spectroscopy (SEM-EDX, see SI) showed that the fused

20 quartz consists of particles ranging from several hundred nm to several µm diameter, composed of Si and O only (detection limit of 0.1 %). Fumed silica was found to have a fractal morphology similar to MSPs and previous microscopy images of fumed silica (Bogdan et al., 2003). MSP analogue suspensions were made up with concentrations of 2.512 ± 0.019 wt% of each analogue.

Meteorite samples were purchased from meteorite-market.com. Detailed characterisation of the Chergach and Allende

25 meteorites can be found in our previous work (James et al., 2017). 8 g of the North West Africa (NWA) 2502 meteorite was ground in an agate ball mill for 1 hour. Chergach (1 g) and Allende (4 g) samples were ground with an agate pestle and mortar. MF analogue suspensions were made up with concentrations of 0.043 ± 0.002 wt% of each analogue.

Fumed silica is manufactured by flame pyrolysis of chemical precursors, typically $SiCl_4$, and was selected as an analogue for MSPs with likely similar fractal morphology. To investigate the possibility that other amorphous silica materials might

30 nucleate with different efficiency, fused quartz, which is manufactured by melting and flash freezing of quartz or silica, was also used. Very limited information is available on the specifics of these materials from the manufacturers. Hence, we conducted our own analysis with Powder X-Ray Diffraction (XRD). We used a Bruker D8 to confirm that both materials are

amorphous. $MgFeSiO_4$ particles synthesised in our laboratory (James et al., 2017) were used as an analogue for MSPs without significant alteration by acid droplets.

The three meteorite samples were chosen as analogues for MFs since they contained fine-grained particles of relevant phases (Taylor et al., 2012;James et al., 2017). The Allende CV3 meteorite has been used widely in the literature as an analogue for

5   interplanetary dust and ablating meteors (Gómez-Martín et al., 2017;Clarke et al., 1971); it is distinct in that it contains significant calcium / aluminium inclusions. NWA is also a carbonaceous CV3 type meteorite and is known to contain significant magnetite (Russell et al., 2005), identified as a coating of micrometeorites (Biermann et al., 1996). Chergach is an H5 ordinary chondrite and was included here to investigate the possibility that the activity of ground meteorites was due to the organic component; it is also known to contain significant metallic Fe and Ni (Weisberg et al., 2008).

10   **3 Results**

Nucleation of crystalline phases was observed at temperatures relevant to PSCs in droplets of 39.94 ± 0.08 wt% HNO_3 in H_2O. Figure 2 shows the evolution of an array of droplets during an experiment. Nucleation events were observed between 210 and 183 K during cooling by a clear 'darkening' as crystals grew within the droplets. The crystallisation of the droplet occurred in less than one second (the image acquisition rate) to over several seconds and nucleation was taken as the first sign of crystal

15   growth. The onset of melting was observed at 231.2 ± 0.7 K on warming and characterised by a radial gradient in the brightness of the droplets as the droplets melted from outside first. This onset of melting is in agreement with the ice / NAT eutectic, suggesting that the crystals are composed of NAT when they melt and that the experimental temperature control and measurement is robust.

A heterogeneous effect on nucleation was observed when analogues for MSPs or MFs were suspended in the solution, as

20   shown in Figure 3. The fused quartz and NWA meteoritic samples were found to nucleate at significantly warmer temperatures than other samples, with some nucleation observed above the melting point of NAD, T_{NAD}. Nucleation events observed above T_{NAD} can only be achieved by direct nucleation of NAT.

In order to test whether dissolved metal salts, which would be present in atmospheric droplets, could alter the nucleation activity of suspended particles, salts of Fe^{3+} and Mg^{2+} were added to suspensions of fumed silica. No effect on the nucleating

25   temperature was observed. This is in contrast to an earlier study (Wise et al., 2003), which found that freezing of aqueous sulfuric acid solutions increased by up to 10 K when metal salts were added.

The fraction of droplets which nucleate on cooling to a temperature T, $f(T)$, depends on the material which is present and the available surface area, s, of that material in each droplet. Hence, fraction frozen is an experiment specific quantity and cannot be directly related to freezing in the atmosphere. To facilitate application to PSCs and also assess the differing activity of each

30   material, the cumulative number of sites per surface area active at a given saturation, n_s, was calculated by $n_s = -\frac{ln(1-f(T))}{s}$ (Murray et al., 2012). In this approach it is assumed that the number of nucleation events is primarily controlled by the

saturation (or temperature) of the system and that the time dependence of nucleation is of secondary importance. This approximation works well when the active sites across a surface are diverse in their ability to nucleate (Herbert et al., 2014). An alternative, but more complex, approach is to define the spectrum of nucleation sites within the context of CNT where each site has a characteristic contact angle and the freezing probability is summed over the distribution of sites (Hoyle et al.,

5   2013;Niedermeier et al., 2011;Broadley et al., 2012). Hoyle et al. (2013) used such a model to show that when saturation in the atmosphere did not change, the number of NAT crystals only increased marginally. Hence, using n_s to extrapolate experimental data to atmospheric contexts will lead to a slight underestimation of the concentration of NAT particles produced in a cloud.

Figure 4 shows that the materials investigated here have a wide range of activity (n_s) over atmospherically relevant conditions

10   of S_{NAT}. The three ground meteoritic samples (which were selected as they contain a range of different minor component phases, see Sect. 2) have remarkably similar activity when plotted in n_s despite nucleating at significantly different temperatures. This suggests that the major olivine / pyroxene phase may dominate the heterogeneous activity, rather than the carbonaceous, metallic or any other minor mineral component that varies strongly between the three samples. The apparent agreement between the active MSP analogue fused quartz and the meteoritic samples is likely coincidental, since the silicon

15   content of meteorites is dominated by crystalline olivine and pyroxene, whilst silica minerals or amorphous silica phases are negligible (Jessberger et al., 2001). The two remaining amorphous silica materials show remarkably different activity to the other samples. The reasons for this differing activity are unclear, but suggest that relatively small changes in surface properties of materials may have significant impacts on their nucleating activity. Alternatively, the significantly smaller activity of the fumed silica and MgFeSiO₄ may be a result of their morphology. Both have specific surface areas around 200 m² g⁻¹,

20   corresponding to an equivalent spherical radius of 6 nm (Bogdan et al., 2003;James et al., 2017). Such small particles are of a similar order to the size of critical clusters and according to classical nucleation theory are therefore thought to be relatively poor at causing nucleation (Pruppacher and Klett, 1978). In contrast fused quartz has a specific surface area of 4.85 m² g⁻¹, corresponding to spherical particles of 234 nm radius, likely much bigger than the critical cluster.

Since nucleation is observed under conditions where NAD is not thermodynamically stable ($S_{NAD} < 1$), and there is no

25   significant discontinuity in the trend at $S_{NAD} = 1$, it is likely that the nucleation observed here produces NAT directly. Some metastable NAD may form when $S_{NAD} > 1$, however the consistent melting onset of droplets in agreement with the NAT / ice eutectic suggests that any NAD which formed in the atmosphere would convert to NAT. The parameterisations shown in Figure 4 were therefore used to investigate the activity of meteoric material in heterogeneously nucleating PSC formation in the atmosphere.

30   **4 Implications for stratospheric clouds**

In order to assess the heterogeneous nucleation of PSCs by meteoric material, it is necessary to estimate the availability of MFs and MSPs, and the conditions (temperature and concentration of droplets) at the time of nucleation.

4.1 Availability of meteoric material in the stratosphere

Simulations of MSP growth and sedimentation have been carried out in a number of previous studies (Bardeen et al., 2008;Frankland et al., 2015;Neely et al., 2011). For this study we performed Whole Atmosphere Community Climate Model (WACCM, e.g., Marsh et al. (2013)) runs with specified dynamics using the Modern-Era Retrospective Analysis for Research and Applications (MERRA) reanalysis (Rienecker et al., 2011), an MSP input of 7.9 t d^{-1} (Carrillo-Sánchez et al., 2016), and included an interaction between MSP and sulfate aerosol through condensation and heterogeneous nucleation (see supplementary material for details). Aerosol microphysics calculations were performed using the Community Aerosol and Radiation Model for Atmospheres (CARMA) model (Toon et al., 1988;Toon et al., 1979;Turco et al., 1979). The zonal mean MSP density at 67° N and 70 hPa during February, averaged over 2011-2014, is $(1.5 \pm 0.5) \times 10^{-15}$ g cm^{-3}.

If these MSPs were spread evenly among liquid droplets with a concentration of 20 cm^{-3} (number per unit volume of atmosphere), and agglomerate or partially dissolve / precipitate to form one sphere in each droplet, they would have a radius of 20 nm and a total surface area of 0.17 ± 0.04 µm^2 cm^{-3} (surface area of MSP per unit volume of atmosphere). This is a factor of 30 times smaller than assumed in a previous laboratory study (Biermann et al., 1996), while in a more recent modelling study (Hoyle et al., 2013) the assumption of 7.5 cm^{-3} foreign spheres of 20 nm radius results in a surface area around three times smaller than that estimated here.

Since the available surface area of MFs is much more poorly constrained, the surface area of MSPs has been scaled according to the mass ratio of ablated to unablated material (giving a surface area of 0.76 µm^2 cm^{-3}, a factor of 4.5 larger than MSPs) (Carrillo-Sánchez et al., 2016). If fragmentation reduced the size of meteoroids to that of MSPs then they would be subject to atmospheric circulation and focussing in the polar vortex, and would therefore have significant lifetimes in acid droplets and partially dissolve. However, estimates of meteoric input fluxes from the measurements in the stratosphere suggest that the input flux may be higher than that estimated here by a factor of two (Cziczo et al., 2001). The assumption that meteoroids fragment to MSP sizes will produce a larger bias than this uncertainty in mass, so this estimate of surface area is likely an upper limit but is considered physically reasonable for the purposes of this study.

4.2 Atmospheric conditions and impact of heterogeneous nucleation

The nucleation of NAT has been shown here to be extremely sensitive to S_{NAT}, which depends on the temperature and chemical composition of liquid droplets (Clegg et al., 1998). Several case studies, using time independent temperature or an observed atmospheric temperature profile, are now used to investigate the relevance of the measured nucleation activity in the atmosphere. Atmospheric droplet concentrations and saturations are calculated from the Aerosol Inorganic Model (Clegg et al., 1998), and in combination with our experimentally derived $n_s(S)$ the resulting concentration of crystals in a given atmospheric volume, N_{NAT}, are derived. Availability of meteoric materials was taken to be as described above and the initial number concentration of liquid droplets was set to 20 cm^{-3}. Since virtually all H$_2$SO$_4$ at PSC altitudes condenses onto droplets

at temperatures above 200 K, and H$_2$O does not affect saturation until below 194 K, equilibrium droplet concentrations and saturations when nucleation occurs are most sensitive to the available mixing ratio of gas-phase HNO$_3$.

Figure 5 illustrates the predicted N_{NAT} as a function of atmospheric temperature for typical stratospheric mixing ratios of H$_2$SO$_4$, HNO$_3$ and H$_2$O. The plot shows that the MF analogues and the more active MSP analogue have sufficiently large n_s to produce

5 in excess of the atmospheric abundances of NAT crystals at a supercooling of several degrees below the NAT melting point (T_{NAT} ~ 198 K) and at temperatures well above the frost point (i.e. where water ice cannot form). This suggests that both MFs and MSPs have the potential to nucleate NAT in the stratosphere. However, the less active MSP analogues cannot explain the observed number concentrations: determining the applicability of each of these amorphous silica materials as MSP analogues and why some nucleate extremely efficiently while others do not, are topics for future work.

10 Figure 5 also shows that varying the atmospheric concentration of HNO$_3$ within observed limits makes a significant difference to the nucleation activities predicted by the parameterisations from the present study. The saturation in a droplet in equilibrium with the gas phase increases approximately linearly when the available HNO$_3$ is varied from 10-15 ppbv (assuming 5 ppmv H$_2$O and 0.1 ppbv H$_2$SO$_4$). However, this produces a logarithmic increase in n_s, which significantly increases N_{NAT}.

While Figure 5 shows that meteoric materials have the potential to trigger nucleation of NAT under stratospheric conditions,

15 atmospheric trajectories of air parcels tend to be more complex. Figure 6 illustrates the NAT concentration expected for the temperature history taken from an observed cloud (Voigt et al., 2005), where only a modest NAT supersaturation was reached and water ice could not have formed. The equilibrium droplet concentration and resulting saturation was calculated as a function of time for the back trajectory temperatures from the atmospheric measurement (Voigt et al., 2005), assuming a range between 10 and 15 ppbv HNO$_3$. The temperature profile and resulting saturations are shown in Figure 6 (a). The resulting $N_{NAT,}$

20 Figure 6 (b), were then calculated and compared to the atmospheric observations corresponding to the temperature profile. The n_s parameterisations measured here for fused quartz and meteorites are able to reproduce the observed density of NAT crystals.

In Figure 6b, we compare to the constant volume nucleation NAT production rate used by Voigt et al. (2005) and also the CNT based model of Hoyle et al. (2013). These literature models have been tuned to reproduce observed NAT concentrations and so generally produce similar N_{NAT}, but the production of NAT earlier in the cloud's evolution vary markedly. The constant

25 volume nucleation rate (here 8×10^{-6} cm^{-3} hour^{-1}, taken from Voigt et al. (2005)) produces a steep increase in NAT crystal number at relatively low saturations. In contrast, the NAT production based on the n_s parameterisations is much more gradual (it should be noted that the parameterisation is extrapolated to $S_{NAT} = 1$, whereas in reality n_s will tend to zero on approaching $S_{NAT} = 1$). The delay in production of NAT to higher S_{NAT} is consistent with modelling which shows that a temperature bias of 1.5 K on all aerosol processes was found to better reproduce observed ozone when using a constant volume nucleation

30 parameterisation (Brakebusch et al., 2013), although this is likely to arise in part because of biases in the model temperature fields (Solomon et al., 2015). The n_s parameterisations measured here tend to predict nucleation of NAT earlier and with a

more gradual increase than the CNT approach used by Hoyle et al. (2013). Each of these differences could have significant implications for predicted Cl and Br activation, and ultimately ozone depletion.

One major uncertainty, which should be a topic of future work, is the impact of H_2SO_4 on the nucleating ability of these materials. MSPs in particular will be included into H_2SO_4 droplets significantly above the altitudes where PSC form and are thought to be processed chemically in those droplets (Neely et al., 2011;Saunders et al., 2012). Whilst we have used analogues for MSPs after processing, a more complete study would work in ternary solution droplets of atmospherically relevant concentrations. Since covering a significant portion of the phase diagram would be extremely time consuming, and since the methods used here would need to be significantly modified to investigate chemical processing at relevant temperatures, no work on ternary solutions is included here. Further work quantifying the time dependence of nucleation and the availability of MFs in the stratosphere would also allow the production of a parameterisation which could be used to investigate heterogeneous nucleation of PSCs in global models. Neverthless, we demonstrate here - for the first time - that meteoric materials have the potential to nucleate NAT particles under stratospheric conditions.

5 Conclusions

Heterogeneous nucleation by analogues for Meteoric Smoke Particles (MSPs) and Meteoric Fragments (MFs) in binary HNO_3 / H_2O solutions has been measured in the laboratory. Nitric Acid Trihydrate (NAT) likely formed directly (rather than *via* the dihydrate) under atmospherically relevant saturation conditions. Parameterisations of the resulting activity were used to show that this mechanism is a potential pathway to forming NAT crystals in Polar Stratospheric Clouds (PSCs) of observed number densities in the absence of water ice.

Good agreement between three significantly different meteorites suggests that the nucleating ability is controlled by the bulk olivine / pyroxene phases common to each sample. Striking differences were observed between the amorphous silica analogues, likely due to morphological differences. Further work is required to assess the most appropriate analogue for MSPs.

The parameterisations developed here predict nucleation at cooler temperatures than parameterisations based on a constant nucleation rate per volume, but at warmer temperatures than a recent parameterisation based on classical nucleation theory. All parameterisations were found to be sensitive to assumptions of the available HNO_3. The availability of MFs is also a major uncertainty and future work on PSCs would clearly benefit from a quantified input of meteoric fragments.

It has been shown here that meteoric material, both MSPs and MFs, can trigger nucleation in PSCs. This could have significant implications for future modelling of PSC formation, Cl and Br activation (through differing rates of activation and denitrification) and ultimately ozone destruction.

Data and sample availability

Raw experimental data (including measured BET surface areas) and fit to Voigt et al. (2005) temperature profiles are available in a supplementary file. The available surface areas assumed for MSPs and MFs were taken from a WACCM run which is

described in the supplementary text, data can be obtained on request from JMCP. Data relating to subsequent plots in Sect. 4 may be obtained on request from BJM. Samples of materials used may be obtained (subject to availability) on request from JMCP, or see (James et al., 2017) for further details of the origins and preparation of suitable alternatives.

Supplement Links

5   [Link to supplementary data to be inserted by copernicus]

[Link to supplementary text to be inserted by copernicus]

Author contributions:

ADJ performed all experiments and data analysis and led authorship of this manuscript.

JSAB supplied modelling data which allowed interpretation of the atmospheric implications of the laboratory measurements.

10   TPM assisted with data analysis and interpretation.

TFW advised on selecting silica material analogues and assisted in developing the experimental method.

JMCP assisted with estimates of atmospheric concentrations of meteoric material and supervised the project.

BJM supervised experiments and contributed significantly to interpreting data both in the laboratory and atmospheric contexts.

15   **Competing interests**: The authors declare no competing financial interests

Acknowledgements

This study was funded by the European Research Council (project number 291332 - CODITA). We would also like to thank Prof. Martyn Chipperfield and Prof. Margaret Campbell-Brown for insightful discussions.

References

20

Bardeen, C. G., Toon, O. B., Jensen, E. J., Marsh, D. R., and Harvey, V. L.: Numerical simulations of the three-dimensional distribution of meteoric dust in the mesosphere and upper stratosphere, J. Geophys. Res.: Atmos., 113, D17202, 2008.
Biermann, U. M., Presper, T., Koop, T., Mößinger, J., Crutzen, P. J., and Peter, T.: The unsuitability of meteoritic and other nuclei for polar stratospheric cloud freezing, Geophys. Res. Lett., 23, 1693-1696, 10.1029/96gl01577, 1996.
25   Bogdan, A., Molina, M. J., Kulmala, M., MacKenzie, A. R., and Laaksonen, A.: Study of finely divided aqueous systems as an aid to understanding the formation mechanism of polar stratospheric clouds: Case of HNO$_3$/H$_2$O and H$_2$SO$_4$/H$_2$O systems, J. Geophys. Res.: Atmos., 108, 4302, 10.1029/2002JD002605, 2003.
Brakebusch, M., Randall, C. E., Kinnison, D. E., Tilmes, S., Santee, M. L., and Manney, G. L.: Evaluation of Whole Atmosphere Community Climate Model simulations of ozone during Arctic winter 2004–2005, J. Geophy. Res.: Atmos., 118, 2673-2688, 10.1002/jgrd.50226, 2013.
30   Broadley, S. L., Murray, B. J., Herbert, R. J., Atkinson, J. D., Dobbie, S., Malkin, T. L., Condliffe, E., and Neve, L.: Immersion mode heterogeneous ice nucleation by an illite rich powder representative of atmospheric mineral dust, Atmos. Chem. Phys., 12, 287-307, 10.5194/acp-12-287-2012, 2012.

Carrillo-Sánchez, J. D., Nesvorný, D., Pokorný, P., Janches, D., and Plane, J. M. C.: Sources of cosmic dust in the Earth's atmosphere, Geophys. Res. Lett., 43, 11,979-911,986, 10.1002/2016GL071697, 2016.

Clarke, R., Jarosevich, E., Mason, B., Nelen, J., Gomez, M., and Hyde, J. R.: The Allende, Mexico, Meteoroite Shower, Smithsonian Institution Press, Washington, 1971.

5 Clegg, S. L., Brimblecombe, P., and Wexler, A. S.: Thermodynamic model of the system $H^+−NH_4^+−SO_4^{2-}−NO_3^-−H_2O$ at tropospheric temperatures, J. Phys. Chem. A, 102, 2137-2154, 10.1021/jp973042r, 1998.

Cziczo, D. J., Thomson, D. S., and Murphy, D. M.: Ablation, flux, and atmospheric implications of meteors inferred from stratospheric aerosol, Science, 291, 1772-1775, 10.1126/science.1057737, 2001.

Dhomse, S. S., Saunders, R. W., Tian, W., Chipperfield, M. P., and Plane, J. M. C.: Plutonium-238 observations as a test of modeled transport
10 and surface deposition of meteoric smoke particles, Geophys. Res. Lett., 40, 4454-4458, 2013.

Frankland, V. L., James, A. D., Feng, W., and Plane, J. M. C.: The uptake of HNO_3 on meteoric smoke analogues, J. Atmos. Sol.-Terr. Phys., 127, 150-160, http://dx.doi.org/10.1016/j.jastp.2015.01.010, 2015.

Gómez-Martín, J. C., Bones, D. L., Carrillo-Sánchez, J. D., James, A. D., Trigo-Rodríguez, J. M., B. Fegley, J., and Plane, J. M. C.: Novel experimental simulations of the atmospheric injection of meteoric metals, Astrophys. J., 836, 212, 2017.

15 Grothe, H., Tizek, H., and Ortega, I. K.: Metastable nitric acid hydrates-possible constituents of polar stratospheric clouds?, Faraday Disc., 137, 223-234, 2008.

Harrison, A. D., Whale, T. F., Carpenter, M. A., Holden, M. A., Neve, L., O'Sullivan, D., Vergara Temprado, J., and Murray, B. J.: Not all feldspars are equal: a survey of ice nucleating properties across the feldspar group of minerals, Atmos. Chem. Phys., 16, 10927-10940, 10.5194/acp-16-10927-2016, 2016.

20 Herbert, R. J., Murray, B. J., Whale, T. F., Dobbie, S. J., and Atkinson, J. D.: Representing time-dependent freezing behaviour in immersion mode ice nucleation, Atmos. Chem. Phys., 14, 8501-8520, 10.5194/acp-14-8501-2014, 2014.

Hoyle, C. R., Engel, I., Luo, B. P., Pitts, M. C., Poole, L. R., Grooß, J. U., and Peter, T.: Heterogeneous formation of polar stratospheric clouds – Part 1: Nucleation of Nitric Acid Trihydrate (NAT), Atmos. Chem. Phys., 13, 9577-9595, 2013.

James, A. D., Frankland, V. L. F., Trigo-Rodríguez, J. M., Alonso-Azcárate, J., Gómez Martín, J.-C., and Plane, J. M. C.: Synthesis and
25 characterisation of analogues for interplanetary dust and meteoric smoke particles, J. Atmos. Sol.-Terr. Phys., 162, 178-191, https://doi.org/10.1016/j.jastp.2016.08.011, 2017.

Jessberger, E. K., Stephan, T., Rost, D., Arndt, P., Maetz, M., Stadermann, F. J., Brownlee, D. E., Bradley, J. P., and Kurat, G.: Properties of interplanetary dust: information from collected samples, in: Interplanetary Dust, edited by: Grün, E., Gustafson, B. Å. S., Dermott, S., and Fechtig, H., Springer Berlin Heidelberg, Berlin, Heidelberg, 253-294, 2001.

30 Lambert, A., Santee, M. L., and Livesey, N. J.: Interannual variations of early winter Antarctic polar stratospheric cloud formation and nitric acid observed by CALIOP and MLS, Atmos. Chem. Phys., 16, 15219-15246, 10.5194/acp-16-15219-2016, 2016.

Langowski, M. P., von Savigny, C., Burrows, J. P., Feng, W., Plane, J. M. C., Marsh, D. R., Janches, D., Sinnhuber, M., Aikin, A. C., and Liebing, P.: Global investigation of the Mg atom and ion layers using SCIAMACHY/Envisat observations between 70 and 150 km altitude and WACCM-Mg model results, Atmos. Chem. Phys., 15, 273-295, 10.5194/acp-15-273-2015, 2015.

35 Mann, G. W., Carslaw, K. S., Chipperfield, M. P., Davies, S., and Eckermann, S. D.: Large nitric acid trihydrate particles and denitrification caused by mountain waves in the Arctic stratosphere, J. Geophys. Res.: Atmos., 110, 10.1029/2004JD005271, 2005.

Marsh, D. R., Mills, M. J., Kinnison, D. E., Lamarque, J. F., Calvo, N., and Polvani, L. M.: Climate Change from 1850 to 2005 Simulated in CESM1 (WACCM), J. Clim., 26, 7372-7391, 10.1175/jcli-d-12-00558.1, 2013.

Meilinger, S. K., Koop, T., Luo, B. P., Huthwelker, T., Carslaw, K. S., Krieger, U., Crutzen, P. J., and Peter, T.: Size-dependent stratospheric
40 droplet composition in Lee wave temperature fluctuations and their potential role in PSC freezing, Geophys. Res. Let., 22, 3031-3034, 10.1029/95GL03056, 1995.

Murphy, D. M., Froyd, K. D., Schwarz, J. P., and Wilson, J. C.: Observations of the chemical composition of stratospheric aerosol particles, Quart. J. Royal Met. Soc., 140, 1269-1278, 2014.

Murray, B. J., O'Sullivan, D., Atkinson, J. D., and Webb, M. E.: Ice nucleation by particles immersed in supercooled cloud droplets, Chem.
45 Soc. Rev., 41, 6519-6554, 10.1039/C2CS35200A, 2012.

Neely, R. R., English, J. M., Toon, O. B., Solomon, S., Mills, M., and Thayer, J. P.: Implications of extinction due to meteoritic smoke in the upper stratosphere, Geophys. Res. Lett., 38, L24808, 10.1029/2011gl049865, 2011.

Niedermeier, D., Hartmann, S., Clauss, T., Wex, H., Kiselev, A., Sullivan, R. C., DeMott, P. J., Petters, M. D., Reitz, P., Schneider, J., Mikhailov, E., Sierau, B., Stetzer, O., Reimann, B., Bundke, U., Shaw, R. A., Buchholz, A., Mentel, T. F., and Stratmann, F.: Experimental
50 study of the role of physicochemical surface processing on the IN ability of mineral dust particles, Atmos. Chem. Phys., 11, 11131-11144, 10.5194/acp-11-11131-2011, 2011.

Peter, T., and Grooß, J. U.: Chapter 4: Polar stratospheric clouds and sulfate aerosol particles: Microphysics, denitrification and heterogeneous chemistry, in: Stratospheric Ozone Depletion and Climate Change, The Royal Society of Chemistry, 108-144, 2012.

Pruppacher, H. R., and Klett, J. D.: Microphysics of clouds and precipitation, D. Reidel Publishing Company, Dordretch, Holland, 1978.

55 Rienecker, M. M., Suarez, M. J., Gelaro, R., Todling, R., Bacmeister, J., Liu, E., Bosilovich, M. G., Schubert, S. D., Takacs, L., Kim, G. K., Bloom, S., Chen, J. Y., Collins, D., Conaty, A., Da Silva, A., Gu, W., Joiner, J., Koster, R. D., Lucchesi, R., Molod, A., Owens, T., Pawson,

S., Pegion, P., Redder, C. R., Reichle, R., Robertson, F. R., Ruddick, A. G., Sienkiewicz, M., and Woollen, J.: MERRA: NASA's Modern-Era Retrospective Analysis for Research and Applications, J. Clim., 24, 3624-3648, 10.1175/jcli-d-11-00015.1, 2011.

Russell, S. S., Zolensky, M., Righter, K., Folco, L., Jones, R., Connolly, H. C., Grady, M. M., and Grossman, J. N.: The meteoritical bulletin, No. 89, 2005 September, Meteorit. Plan. Sci., 40, A201-A263, 10.1111/j.1945-5100.2005.tb00425.x, 2005.

5   Saunders, R. W., and Plane, J. M. C.: A laboratory study of meteor smoke analogues: Composition, optical properties and growth kinetics, J. Atmos. Sol.-Terr. Phys., 68, 2182-2202, http://dx.doi.org/10.1016/j.jastp.2006.09.006, 2006.

Saunders, R. W., Dhomse, S., Tian, W. S., Chipperfield, M. P., and Plane, J. M. C.: Interactions of meteoric smoke particles with sulfuric acid in the Earth's stratosphere, Atmos. Chem. Phys., 12, 4387-4398, 10.5194/acp-12-4387-2012, 2012.

Solomon, S.: Stratospheric ozone depletion: A review of concepts and history, Rev. Geophys., 37, 275-316, 10.1029/1999RG900008, 1999.

10   Solomon, S., Kinnison, D., Bandoro, J., and Garcia, R.: Simulation of polar ozone depletion: An update, J. Geophys. Res.: Atmos., 120, 7958-7974, 10.1002/2015JD023365, 2015.

Subasinghe, D., Campbell-Brown, M. D., and Stokan, E.: Physical characteristics of faint meteors by light curve and high-resolution observations, and the implications for parent bodies, Mon. Not. Royal Astro. Soc., 457, 1289-1298, 2016.

Taylor, S., Matrajt, G., and Guan, Y.: Fine-grained precursors dominate the micrometeorite flux, Meteorit. Planet. Sci., 47, 550-564,
15   10.1111/j.1945-5100.2011.01292.x, 2012.

Toon, O. B., Turco, R. P., Hamill, P., Kiang, C. S., and Whitten, R. C.: One-dimensional model describing aerosol formation and evolution in the stratosphere. 2. Sensitivity studies and comparison with observations, J. Atmos. Sci., 36, 718-736, 10.1175/1520-0469(1979)036<0718:aodmda>2.0.co;2, 1979.

Toon, O. B., Turco, R. P., Westphal, D., Malone, R., and Liu, M.: A Multidimensional Model for Aerosols: Description of Computational
20   Analogs, J. Atmos. Sci., 45, 2123-2144, 10.1175/1520-0469(1988)045<2123:ammfad>2.0.co;2, 1988.

Turco, R. P., Hamill, P., Toon, O. B., Whitten, R. C., and Kiang, C. S.: One-dimensional model describing aerosol formation and evolution in the stratosphere. 1. Physical processes and mathematical analogs, J. Atmos. Sci., 36, 699-717, 10.1175/1520-0469(1979)036<0699:aodmda>2.0.co;2, 1979.

Voigt, C., Schlager, H., Luo, B. P., Dörnbrack, A., Roiger, A., Stock, P., Curtius, J., Vössing, H., Borrmann, S., Davies, S., Konopka, P.,
25   Schiller, C., Shur, G., and Peter, T.: Nitric Acid Trihydrate (NAT) formation at low NAT supersaturation in Polar Stratospheric Clouds (PSCs), Atmos. Chem. Phys., 5, 1371-1380, 10.5194/acp-5-1371-2005, 2005.

Wegner, T., Grooß, J. U., von Hobe, M., Stroh, F., Sumińska-Ebersoldt, O., Volk, C. M., Hösen, E., Mitev, V., Shur, G., and Müller, R.: Heterogeneous chlorine activation on stratospheric aerosols and clouds in the Arctic polar vortex, Atmos. Chem. Phys., 12, 11095-11106, 10.5194/acp-12-11095-2012, 2012.

30   Weisberg, M. K., Smith, C., Benedix, G., Folco, L., Righter, K., Zipfel, J., Yamaguchi, A., and Aoudjehane, H. C.: The Meteoritical Bulletin, No. 94, September 2008, Meteorit. Planet. Sci., 43, 1551-1584, 10.1111/j.1945-5100.2008.tb01027.x, 2008.

Whale, T. F., Murray, B. J., O'Sullivan, D., Wilson, T. W., Umo, N. S., Baustian, K. J., Atkinson, J. D., Workneh, D. A., and Morris, G. J.: A technique for quantifying heterogeneous ice nucleation in microlitre supercooled water droplets, Atmos. Meas. Tech., 8, 2437-2447, 10.5194/amt-8-2437-2015, 2015.

35   Wise, M. E., Brooks, S. D., Garland, R. M., Cziczo, D. J., Martin, S. T., and Tolbert, M. A.: Solubility and freezing effects of Fe^{2+} and Mg^{2+} in H_2SO_4 solutions representative of upper tropospheric and lower stratospheric sulfate particles, J. Geophys. Res.: Atmos., 108, 4434, 10.1029/2003JD003420, 2003.

Figures
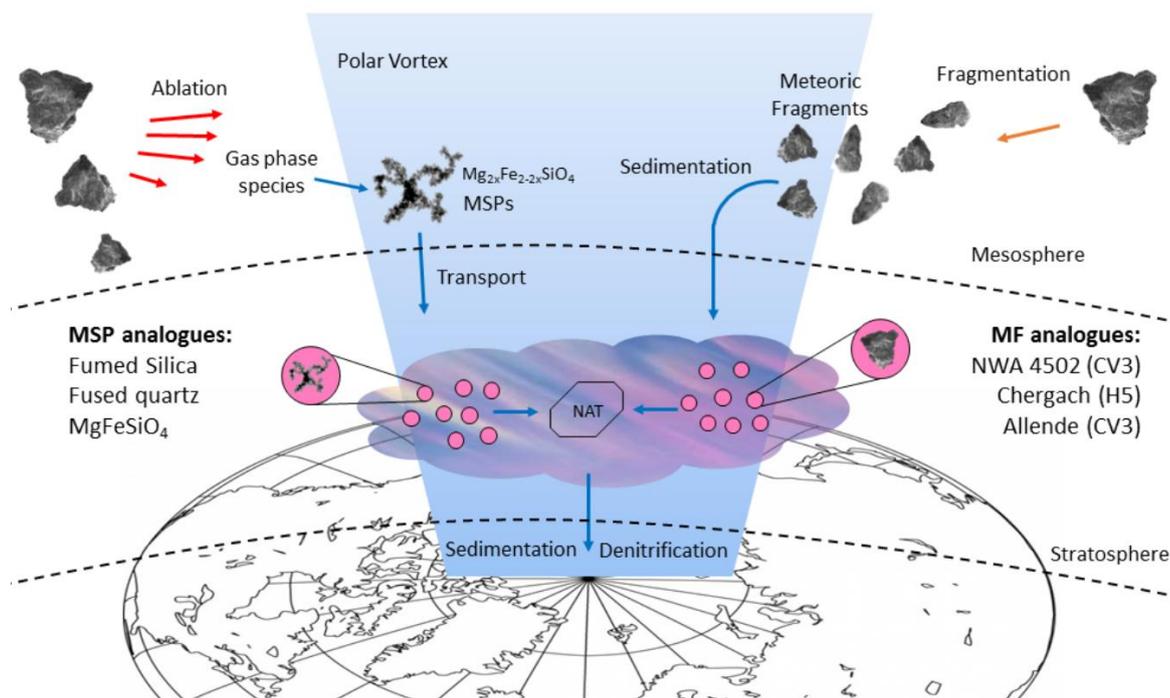
Figure 1: The pathways of two kinds of meteoric material through the atmosphere. Processes are shown which lead to formation of Meteoric Smoke Particles (MSPs) and Meteoric Fragments (MFs), either of which could heterogeneously nucleate Nitric Acid Trihydrate (NAT) in polar stratospheric clouds.
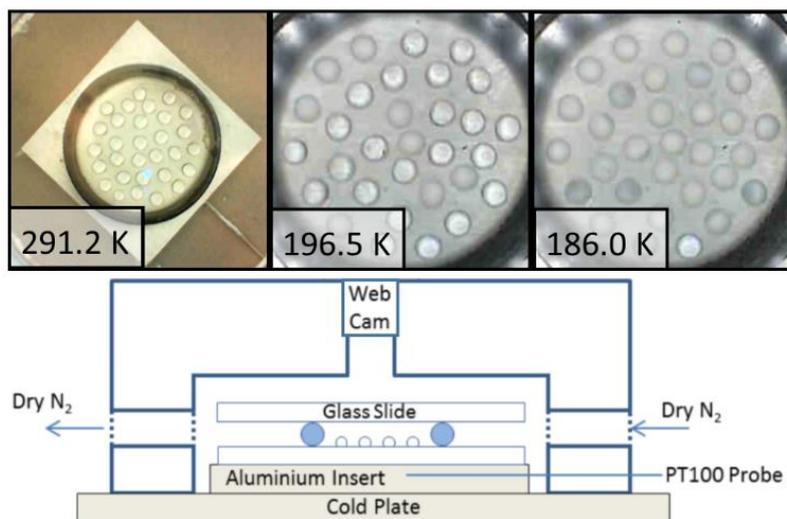
Figure 2: Droplet array on cooling, demonstrating that crystallisation and therefore nucleation temperatures can be distinguished. Panel at room temperature shows the supporting cold plate, aluminium insert with PT100 temperature probe and slide / spacer / slide cell configuration. Panels below room temperature show nucleation events for a 39.98 wt% HNO_3 solution with 0.045 wt% of ground Chergach meteorite particles in suspension (in one droplet shown in the lower right, no nucleation was observed even at 186 K). A side on schematic diagram of the apparatus is also shown (see Sect. 2).
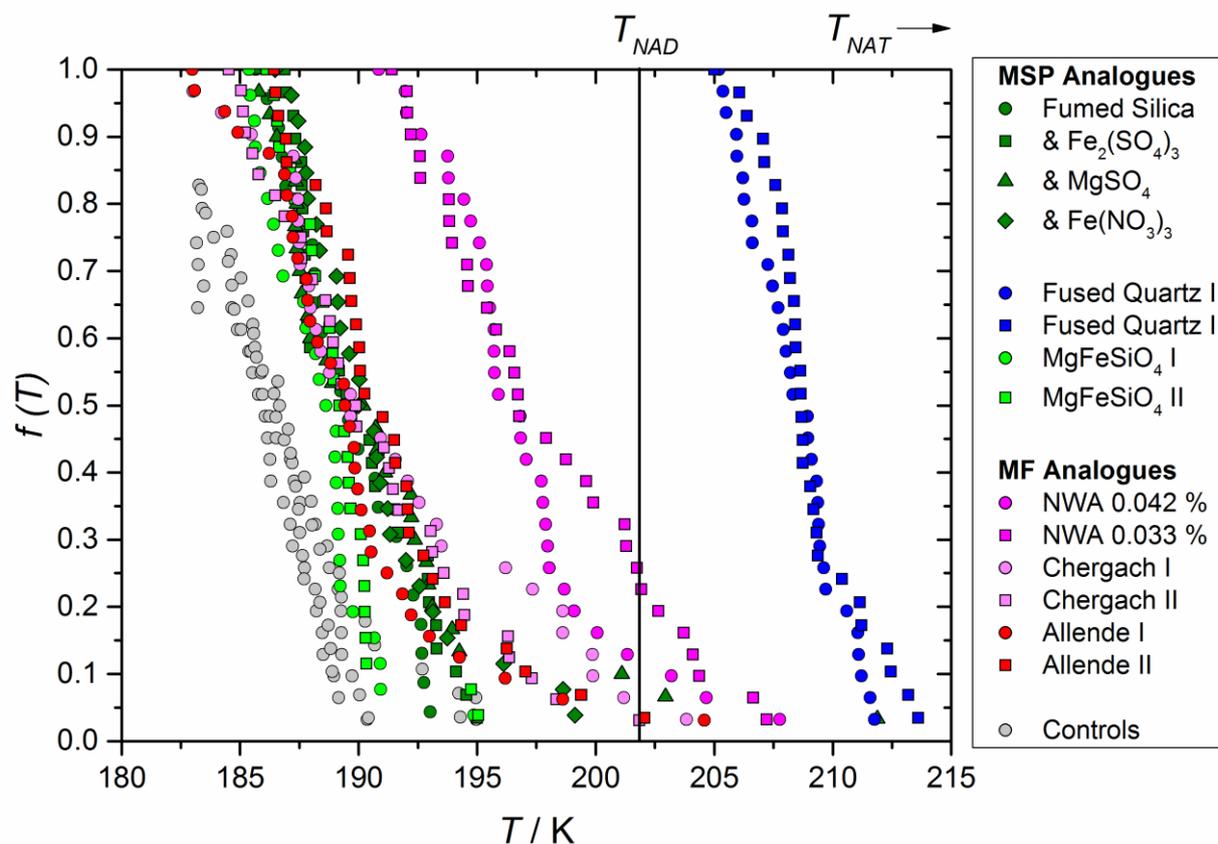
Figure 3: Fraction of droplets crystallised at different temperatures showing a heterogeneous effect for a variety of analogues for MSPs and MFs. Experiments were carried out using particulate solids suspended in 39.94 ± 0.08 wt% HNO₃ in H₂O. MSP analogues are shown in blue and green colours and were suspended to concentrations of 2.512 ± 0.019 wt%, MF analogues are shown in pink and red colours and were suspended in concentrations of 0.043 ± 0.002 wt% except where stated in the legend for the NWA meteorite. Repeat experiments, distinguished by roman numerals, are shown as different symbol shapes. Experiments with fumed silica labelled with metal salts contained 0.635 ± 0.005 wt% of the relevant metal ion as well as fumed silica. The instrument background (when no heterogeneous material was added to the nitric acid solution) measured in four repeat experiments is shown as grey points. A vertical line is used to show the NAD melting point (T_{NAD}), whereas the NAT melting point (T_{NAT}) was at 244 K.
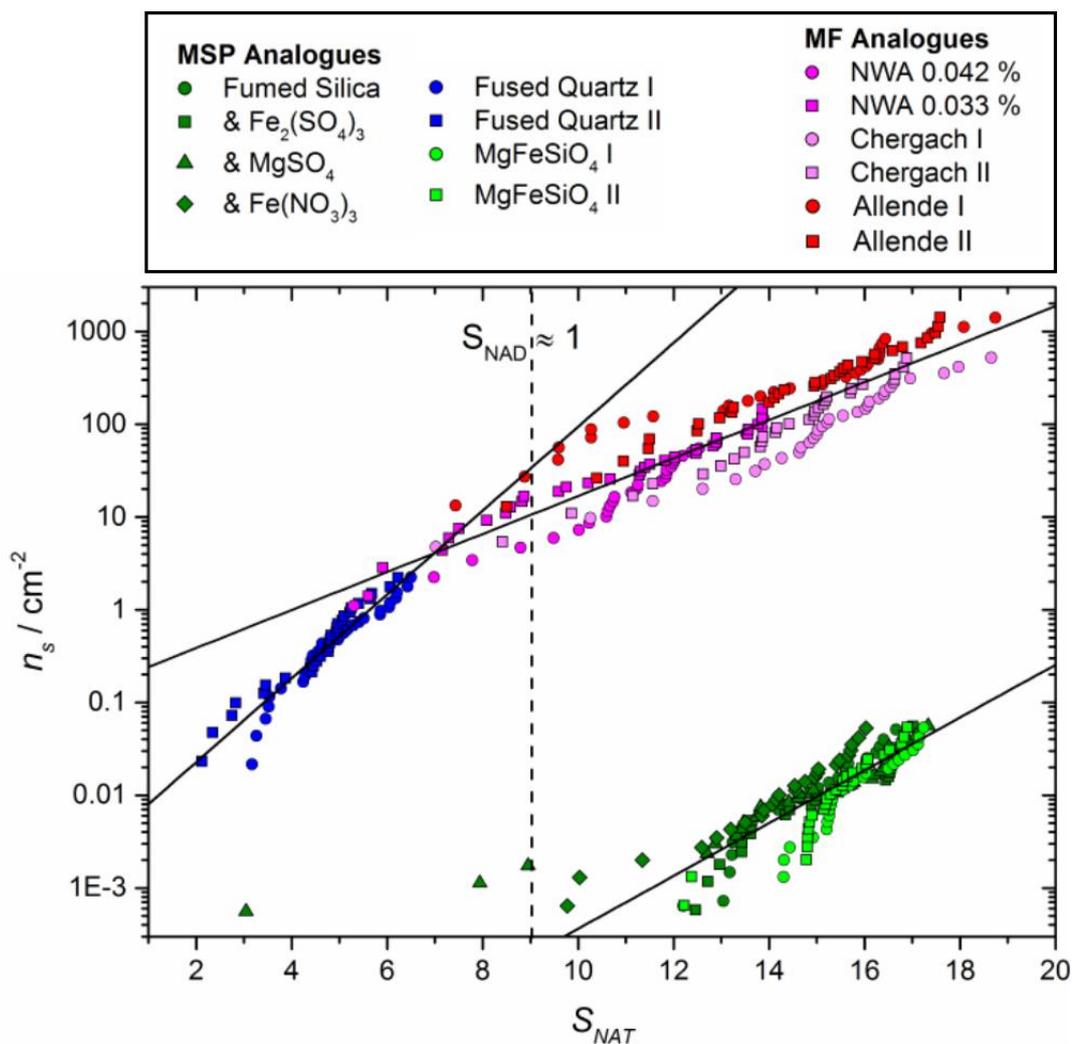
Figure 4: Nucleation activity of MSP and MF analogues investigated here expressed as active sites per unit surface area (n_s) as a function of S_{NAT}. The vertical dashed line shows the approximate position of NAD saturation. Samples were selected and their BET surface areas measured as analogues for both MSPs (Fused Quartz: 4.85 ± 0.06 m^2 g^{-1}, Fumed Silica: 195 ± 3 m^2 g^{-1}, MgFeSiO$_4$: 208 ± 2 m^2 g^{-1}) and MFs (NWA 2502 (CV3): 5.75 ± 0.05 m^2 g^{-1}, Chergach (H5): 0.44 ± 0.14 m^2 g^{-1}, Allende (CV3): 1.22 ± 0.15 m^2 g^{-1}). Log-linear fits have been added as a guide to the eye and to facilitate comparison with atmospheric conditions.
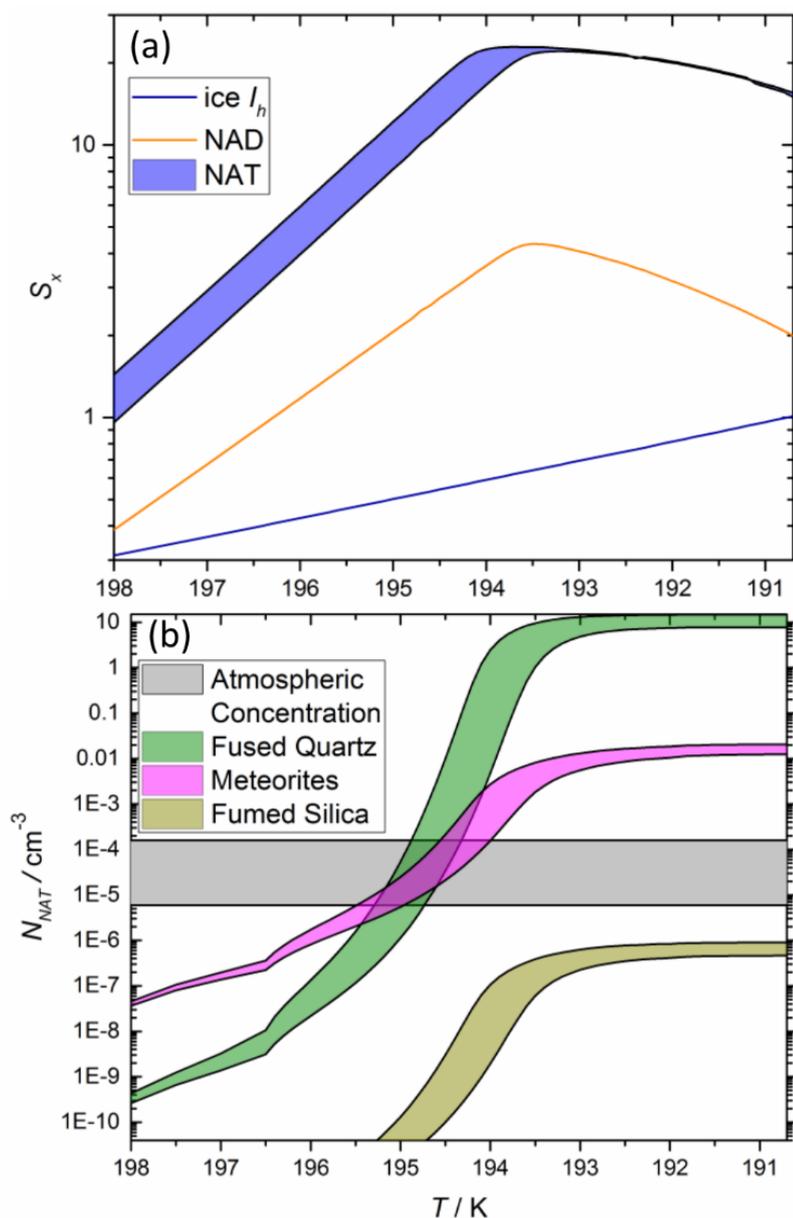
Figure 5: Plot demonstrating that the parameterised nucleating activities of meteoric materials are able to reproduce typical cloud NAT particle concentrations. Saturations with respect to relevant crystalline phases are shown in panel (a) and number concentration is shown in panel (b). Equilibrium saturation ratios were calculated for air masses containing 5 ppmv H_2O, 0.1 ppbv H_2SO_4 and either 10 (minimum of ranges) or 15 ppbv (maximum of ranges) HNO_3 using the Aerosol Inorganic Model (Clegg et al., 1998), and number concentrations were calculated using the n_s parameterisations shown in Figure 4, assuming 20 liquid droplets cm^{-3} air and the availability of meteoric materials described in Sect. 4 of the text.
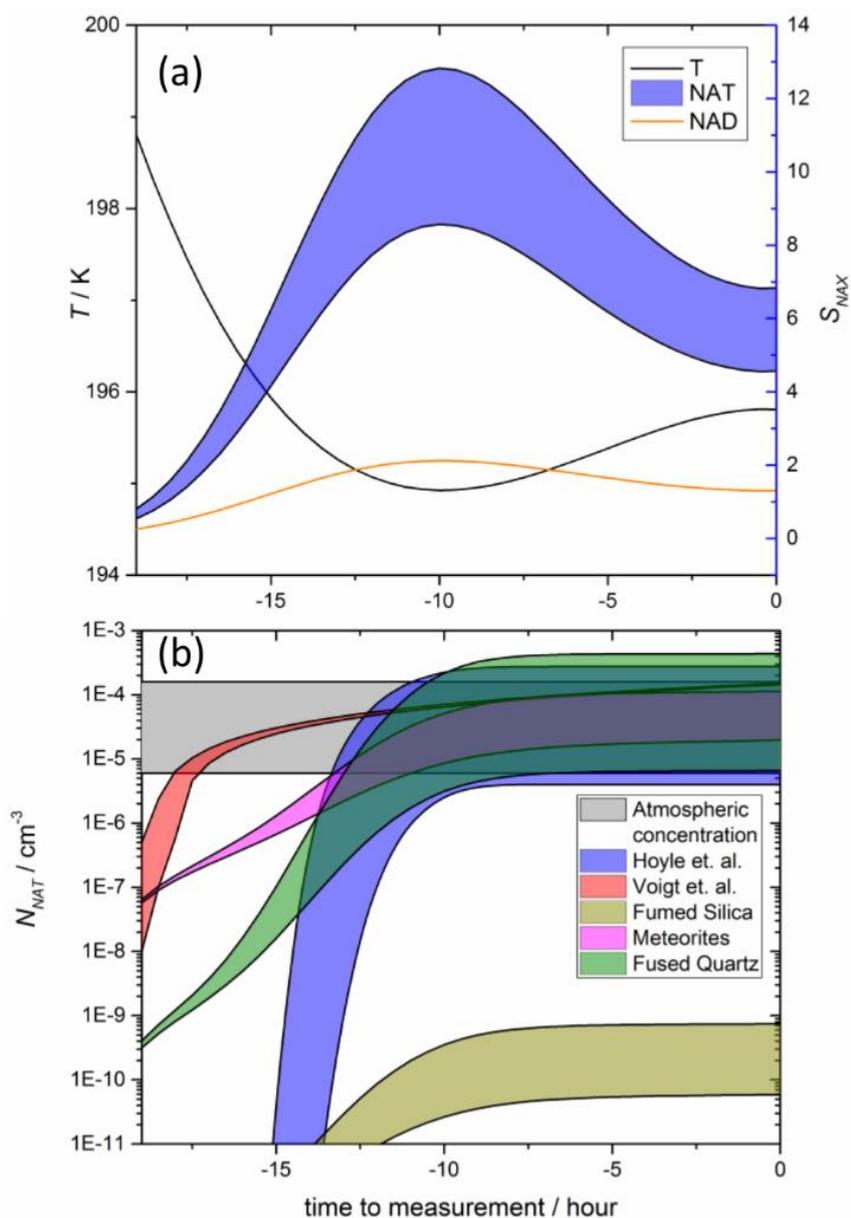
Figure 6: NAT particle production using a temperature trajectory based on stratospheric observations. Temperature profile (a) was taken from back trajectories which ended in cloud with observed N_{NAT} shown in the grey shaded area (b)(Voigt et al., 2005). Saturations shown in (a) were calculated assuming 5 ppmv H_2O, 0.1 ppbv H_2SO_4 and 10 (minimum of ranges) to 15 ppbv (maximum of ranges) HNO_3. No other processes (e.g. growth or sedimentation of particles) are taken into account. (b) shows predicted N_{NAT} based on our n_s parameterisations and estimated surface areas of meteoric material as well as two literature parameterisations (Hoyle et al., 2013;Voigt et al., 2005).